

An Analytic Algorithm to Calculate the Inclination, Ascending Node, and Semimajor Axis of Spectroscopic Binary Orbits Using a Single Speckle Measurement and the Parallax*

J. A. Docobo^{1,2**}, P. P. Campo¹, M. Andrade^{1,3}, and E. P. Horch⁴

¹*R. M. Aller Astronomical Observatory, University of Santiago de Compostela, Santiago de Compostela, 15782 Spain*

²*Faculty of Mathematics, University of Santiago de Compostela, Santiago de Compostela, 15782 Spain*

³*Higher Polytechnic School, University of Santiago de Compostela, Lugo, 27002 Spain*

⁴*Southern Connecticut State University, New Haven, CT 06515 USA*

Received July 11, 2014; in final form, September 17, 2014

Abstract—It is well known that in spectroscopic binary orbits, the inclination, the ascending node, and the semimajor axis remain undetermined, therefore the principal objective of this research is to establish an analytic methodology for the calculation of these parameters for spectroscopic binaries, both single-lined (SB1) and double-lined (SB2). In other words, the goal is to determine their “three-dimensional” orbits using a single speckle measurement (ρ , θ , t) and the parallax (π). Moreover, estimates of the individual masses of each system can also be obtained. The proposed algorithm was successfully applied to SB1 systems: YSC 148 (HD 37393) and CHR 225 (HD 34318), and SB2 systems: LSC 1 Aa1,2 (HD 200077) and Mkt 11 Aa, Ab (HD 358). In this late case, previously determined spectroscopic and visual orbits have been used to compare and contrast the results obtained from them with our results. The methodology presented is especially interesting for those cases in which it is only possible to resolve the spectroscopic binary in the zones of maximum angular separation by optical means thereby making it impossible to avail of sufficient observations in order to calculate the visual orbit.

DOI: 10.1134/S1990341314040087

Keywords: *techniques: high angular resolution—techniques: interferometric—binaries: general*

1. INTRODUCTION

It is well known that double stars constitute a fundamental source of information concerning various stellar parameters, above all that of masses. Based on the orbits of the visual binaries (defined by seven orbital elements: the period, the periastron passage, the eccentricity, the semimajor axis in arcseconds, the inclination, the angle of the node, and the argument of the periastron) and knowing the parallax of the system, it is possible to determine the sum of the masses of the components using Kepler’s third law. Nevertheless, only in a few cases in which the orbits are available with respect to the center of mass, is it possible to separately deduce the mass of each component.

In this sense, it should be said that the quality of the parallaxes today (as measured by the Hipparcos astrometric satellite with a precision superior to

those available earlier), along with the orbital semimajor axes and the periods, have allowed the calculation of the total mass for many systems with much smaller uncertainties than previously possible which, undoubtedly, will be improved by the results of the Gaia mission.

Likewise, empirical calibrations have been established in the last decades that permit researchers to obtain the quotient of the masses from the difference of magnitude of the components (for example, see [1–4]) which, in the case of not having additional information, assists with the calculation of the individual masses at least for concrete luminosity classes.

The spectroscopic double-lined binaries (SB2) allow the deduction of the quotient of the masses of the components based on their orbits. On the other hand, for those single-lined (SB1), one can only achieve an estimate of said coefficient by means of the so-called mass function. In the spectroscopic orbits (calculated from the radial velocities), contrary to the visual binaries, both the inclination and the angle of the node are

*The text was submitted by the authors in English.

**E-mail: joseange1.docobo@usc.es

unknown, and the semimajor axis is given in km but multiplied by the sine of the inclination.

It is clear that if we know both the visual as well as the double lined spectroscopic orbit, we would have not only the complete set of orbital elements but also the individual masses and, moreover, the value of the parallax (orbital parallax) obtained directly from the semimajor axis expressed in arcseconds (from the visual orbit) and in astronomical units (deduced from the spectroscopic orbit and from the inclination of the visual orbit).

For this reason, since researchers began to manage high resolution techniques such as speckle interferometry (for example, [5–12]) at the beginning of the '70s, there has been a clear objective to try to optically resolve spectroscopic binaries with the goal of obtaining maximum information about the components of these stellar systems. The work of these pioneers has been continued by a long list of other researchers, achieving the resolution of spectroscopic binaries using innovative techniques.

Nevertheless, cases may occur in which it is only possible to resolve the spectroscopic binary in zones of maximum angular separation (very inclined orbits, orbits with high eccentricity, etc.) which makes it impossible to have sufficient observations available in order to calculate the visual orbit.

Especially in situations such as above, but also in general, a mathematical problem arises. It deals with calculating the inclination, the ascending node, and the semimajor axis in arcseconds using only the necessary and sufficient data, e.g., an angle of position θ with its corresponding angular separation ρ , and the parallax π , the first two obtained by means of a high precision speckle measurement.

Moreover, the data associated with the magnitude difference of the components $\Delta m = m_2 - m_1$, also given by the speckle register, will be utilized to evaluate the quotient of the masses of the components in the case of single-lined spectroscopic binaries.

In order to resolve the proposed problem, we present an analytic algorithm that we have successfully tested in cases in which the inclination, the node, and the semimajor axis have been previously determined from the visual and spectroscopic orbits of these systems.

The present article is structured in the following manner. The Introduction is followed by Section 2 that presents the notation utilized and the original algorithm proposed. We apply the method to four real cases (Section 3). The first two (Sections 3.1 and 3.2) correspond to single-lined spectroscopic binaries. On the other hand, the other two (Sections 3.3 and 3.4) deal with double-lined spectroscopic binaries. Finally, the conclusions of this research are discussed in Section 4.

2. THE PROPOSED ALGORITHM

As usual, we will use the following terminology to refer to the orbital elements, masses, magnitudes, and other variables and parameters:

- M_i , mass of component i ($i = 1$ for the primary star, $i = 2$ for the secondary star);
- $\alpha = \frac{M_1}{M_2}$;
- m_i , visual magnitude of component i ;
- π , parallax in arcseconds;
- P , orbital period;
- T , epoch of passage of the periastron;
- e , eccentricity;
- a_i , semimajor axis of the orbit of component i with respect to the center of masses (a_i'' in arcseconds, \bar{a}_i in units of distance);
- $\bar{A}_i = \bar{a}_i \sin I$;
- a , semimajor axis of the relative orbit (a'' in arcseconds, \bar{a} in units of distance);
- I , inclination;
- Ω , angle of the ascending node;
- ω_i , argument of the periastron of the orbit of component i with respect to the center of mass;
- t , independent variable “time”;
- M, E, f , mean, eccentric, and true anomalies respectively;
- r , radius vector between the stars;
- θ , angle of position;
- ρ , angular separation.

A single-lined spectroscopic binary whose combined spectrum as well as its orbit is known will be given by the elements: P, T, e, \bar{A}_1 , and ω_1 .

Once a certain value of α is fixed as a function of the spectral type and of the difference of magnitude between the components, for each value of I we calculate the semimajor axis \bar{a}_1 by means of $\bar{a}_1 = \frac{\bar{A}_1}{\sin I}$ and $\bar{a}_2 = \bar{a}_1 \alpha$, therefore $\bar{a} = \bar{a}_1 + \bar{a}_2$. Now the expression

$$M_1 + M_2 = \bar{a}^3 \frac{1}{P^2} \quad (1)$$

gives us the sum of the masses of the components that, along with the value utilized for α , yields the separate masses.

The corresponding values of \bar{a}_1 and \bar{a}_2 in arcseconds can be determined by multiplying by the parallax, that is to say, $a''_1 = \pi \bar{a}_1$, $a''_2 = \pi \bar{a}_2$, and therefore $a'' = a''_1 + a''_2$ gives us the semimajor axis of the relative motion in arcseconds. On the other hand, if t is the instant in which the speckle observation (θ, ρ'') has been performed, we calculate the value of f at the same instant (from the mean and eccentric anomalies as usual) and then

$$r'' = \frac{a''(1 - e^2)}{1 + e \cos f}.$$

Finally, taking into account the relations between the coordinates (r, f) in the true orbit and the corresponding coordinates (ρ, θ) in the apparent orbit (see Fig. 1), the results obtained are the known expressions:

$$\begin{aligned} \rho'' \cos(\theta - \Omega) &= r'' \cos(\omega + f), \\ \rho'' \sin(\theta - \Omega) &= r'' \sin(\omega + f) \cos I, \end{aligned} \tag{2}$$

where $\omega = \omega_2 = 180^\circ + \omega_1$.

These last expressions, used in reverse as usually done when visual ephemerides are calculated, permit us to successively determine the angles Ω and I and thereby close the mathematical process. The solution will be that which yields a difference between the calculated and the initial inclinations below a given value. In the case when the solution is not found, another value of α should be used, at first a value close to it, always keeping in mind the known spectral type as well as Δm . Another issue is that the values of \bar{a} (or a''), I , and Ω that complete the tridimensional orbit are those that are given by the solution obtained.

It must be remembered that the value of I enters into the calculation by way of its sine for which we will not initially be able to discriminate between I and $180^\circ - I$, that is, between direct and retrograde motion. In other words, we obtain two possible values for the inclination with their corresponding values of the angle of the node. Nevertheless, this does not affect the determination of the masses, and it may be resolved later by obtaining more speckle measurements in order to define the direction of the orbit.

Obviously, if the spectroscopic binary is the double-lined type, the value of α is given by $\bar{A}_2/\bar{A}_1 = M_1/M_2$ and therefore is initially known from the orbital elements.

Sometimes in practice situations may occur in which no value for any pair (α, I) is found that provides masses that are consistent with the spectral type and the difference of magnitudes. Moreover, it may even occur that there is no inclination for which the initial and the final values coincide. In these cases, the problem may be due to a lack of precision in the

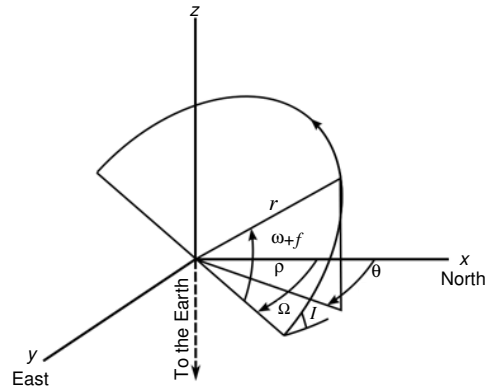


Fig. 1. True and apparent orbits.

speckle measurement, the elements of the spectroscopic orbit, or the parallax.

It may likewise occur that if the speckle observation was performed close to the nodes of the orbit, the expressions (2) give rise to singularities, but this only occurs occasionally. It is avoidable, because the instants when the components pass through the nodes are known to coincide with the maximum and the minimum on the radial velocity curves. In this case, the following procedure must be used. The epoch of passage through the ascending node corresponds to the moment that the radial velocity of the secondary is maximum (or when the radial velocity of the primary is minimum). In this moment, $r = \rho$ and $\Omega = \theta$. In this particular case, the general algorithm must be substituted by

$$\begin{aligned} I &\rightarrow \bar{a} \rightarrow a'', \\ t &\rightarrow M \rightarrow E \rightarrow f \rightarrow r''. \end{aligned}$$

The inclination of the orbit will be the angle for which r and ρ coincide. Note that if the speckle measurement corresponds to the maximum of the radial velocity of the primary, then the ascending node will be $\Omega = 180^\circ - \theta$.

In order to calculate the uncertainties associated with the unknown orbital elements, that is, the angle of the node and the inclination as well as the masses, we have handled all of them as a function of several variables. These comprise a set of intermediate variables: mean, eccentric, and true anomalies as well as distance and semimajor axis in astronomical units. Simultaneously, these are considered as a function of another set of initial variables or data: period, time of periastron passage, eccentricity, argument of the periastron, projected semimajor axis (or supposed masses in the SB1 case), and parallax, in addition to the observed position angle and angular separation for an epoch.

Table 1. Initial results for the YSC 148 system

| Initial value of I , deg | Ω for I , deg | Ω for $180^\circ - I$, deg | Final I , deg | Final $180^\circ - I$, deg | a , arcsec | M_1 , M_\odot | M_2 , M_\odot |
|-------------------------------|---------------------------|---------------------------------------|--------------------|--------------------------------|-----------------|----------------------|----------------------|
| 5 | — | — | — | — | 1.279 | 463.68 | 295.07 |
| 10 | — | — | — | — | 0.642 | 58.63 | 37.31 |
| 15 | 306.6 | 271.6 | 84.8 | 95.2 | 0.431 | 17.71 | 11.27 |
| 20 | 332.9 | 245.3 | 74.0 | 106.0 | 0.326 | 7.67 | 4.88 |
| 25 | 343.3 | 234.8 | 66.4 | 113.6 | 0.264 | 4.07 | 2.59 |
| 30 | 349.5 | 228.7 | 59.5 | 120.5 | 0.223 | 2.46 | 1.56 |
| 35 | 353.6 | 224.6 | 52.9 | 127.1 | 0.194 | 1.63 | 1.03 |
| 40 | 356.5 | 221.7 | 46.2 | 133.8 | 0.173 | 1.16 | 0.73 |
| 45 | 358.7 | 219.5 | 39.4 | 140.6 | 0.158 | 0.87 | 0.55 |
| 50 | 0.3 | 217.9 | 32.3 | 147.7 | 0.145 | 0.68 | 0.43 |
| 55 | 1.6 | 216.6 | 24.4 | 155.6 | 0.136 | 0.56 | 0.35 |
| 60 | 2.5 | 215.7 | 14.6 | 165.4 | 0.129 | 0.47 | 0.30 |
| 65 | 3.3 | 214.9 | — | — | 0.123 | 0.41 | 0.26 |
| 70 | 3.9 | 214.3 | — | — | 0.119 | 0.37 | 0.23 |
| 75 | 4.3 | 213.9 | — | — | 0.115 | 0.34 | 0.22 |
| 80 | 4.6 | 213.6 | — | — | 0.113 | 0.32 | 0.20 |
| 85 | 4.7 | 213.4 | — | — | 0.112 | 0.31 | 0.20 |
| 90 | 4.8 | 213.4 | — | — | 0.111 | 0.31 | 0.19 |

Table 2. Results for the system YSC 148 (second step)

| Initial value of I , deg | Ω for I , deg | Ω for $180^\circ - I$, deg | Final I , deg | Final $180^\circ - I$, deg | a , arcsec | M_1 , M_\odot | M_2 , M_\odot |
|-------------------------------|---------------------------|---------------------------------------|--------------------|--------------------------------|-----------------|----------------------|----------------------|
| 40 | 356.5 | 221.7 | 46.2 | 133.8 | 0.173 | 1.15 | 0.73 |
| 41 | 357.0 | 221.2 | 44.8 | 135.2 | 0.170 | 1.08 | 0.69 |
| 42 | 357.5 | 220.7 | 43.5 | 136.5 | 0.166 | 1.02 | 0.65 |
| 43 | 357.9 | 220.3 | 42.1 | 137.9 | 0.163 | 0.97 | 0.61 |
| 44 | 358.3 | 219.9 | 40.7 | 139.2 | 0.160 | 0.91 | 0.58 |
| 45 | 178.7 | 39.5 | 39.4 | 140.6 | 0.158 | 0.87 | 0.55 |

Table 3. Results with different values of α for the system YSC 148

| α | I , deg | $180^\circ - I$, deg | Ω for I , deg | Ω for $180^\circ - I$, deg | a , arcsec | M_1 , M_\odot | M_2 , M_\odot |
|-------------------|--------------|--------------------------|---------------------------|---------------------------------------|-----------------|----------------------|----------------------|
| 1 | 35 | 145 | 359.5 | 218.7 | 0.151 | 0.63 | 0.63 |
| 1.25 | 39 | 141 | 359.0 | 219.1 | 0.155 | 0.75 | 0.60 |
| $1.0/0.7 = 1.429$ | 41 | 139 | 358.3 | 219.9 | 0.160 | 0.89 | 0.62 |
| $1.2/0.7 = 1.714$ | 44 | 136 | 357.0 | 221.1 | 0.169 | 1.11 | 0.65 |
| 2 | 47 | 133 | 355.9 | 222.3 | 0.178 | 1.36 | 0.68 |
| 2.5 | 52 | 128 | 353.8 | 224.3 | 0.192 | 1.85 | 0.74 |

Then, we assume that the value of each initial/intermediate variable represents the mean of a Gaussian distribution, the corresponding uncertainty being the standard deviation σ . Finally, we propagate uncertainties through a linearized model by using the Taylor series.

3. APPLICATION EXAMPLES

3.1. System YSC 148 = HD 37393 = HIP 27246 = WDS 05465+7437

According to [13], the following orbit exists for this SB1, which has a combined spectrum G0:

$$\begin{aligned}
 P &= 4072^d \pm 91^d = 11.15 \pm 0.25 \text{ yr}, \\
 T &= 49649 \pm 60 \text{ RJD} = 2005.96 \pm 0.16, \\
 e &= 0.326 \pm 0.032, \\
 \bar{A}_1 &= 2.30797 \times 10^8 \pm 9.4 \times 10^6 \text{ km}, \\
 \omega_1 &= 318^\circ.5 \pm 5^\circ.4.
 \end{aligned}$$

This binary was resolved on two occasions by [14], yielding the following values:

| t | θ , deg | ρ , arcsec | Δm |
|-----------|-----------------|-------------------|-----------------|
| 2009.7538 | 289.1 ± 0.9 | 0.154 ± 0.003 | 2.83 ± 0.10 |
| 2009.7647 | 290.1 ± 0.9 | 0.160 ± 0.003 | 3.32 ± 0.14 |

We will begin working with the first measurement, $t = 2009.7538$.

A difference of magnitude of $2^m.83$ can permit us to separate the spectral type G0 in the form F9 V + K4 V that, assuming that both components belong to the main sequence, may yield approximate masses of $1.10 \pm 0.10 M_\odot$ and $0.70 \pm 0.10 M_\odot$. The Hipparcos parallax of this system is $\pi = 28.10 \pm 0.79$ mas.

In this way, we begin the explanation with the parameter $\alpha = 1.57$ ($1.10/0.70$) ± 0.27 . To illustrate the process, we assign values to I every 5° and then, once the solution has been delimited, every 1° .

In Table 1 the results are shown that were obtained by applying the algorithm proposed in Section 2. The corresponding values are listed below.

- First column: initial value of the inclination, taking values at 5° intervals between 0° and 90° .
- Second and third columns: values calculated for the ascending node of the relative orbit for I and for $180^\circ - I$ respectively.
- Fourth and fifth columns: final inclination, values calculated using the algorithm for I and $180^\circ - I$.

- Sixth column: value of the semimajor axis of the relative orbit in arcsec.
- Seventh and eighth columns: values of the obtained individual masses in solar masses.

In Table 1, one can see that the inclination for which the initial and final values coincide is between 40° and 45° (or between 140° and 135°). Refining the interval to 1° , the values presented in Table 2 are obtained.

The solution will be close to 43° . Now, one would be able to continue reducing the interval in order to obtain the solution with increased precision, but given the uncertainties of the entry data, it does not make sense to reach such a high level of precision. Therefore, we can adopt values of $I = 43^\circ \pm 28^\circ$ or $I = 137^\circ \pm 28^\circ$. In this case the uncertainty in the inclination is high because that corresponding to the argument of the periastron (spectroscopic orbit) is quite high, and the propagation of the uncertainties leads to it. Concretely, the uncertainty of ω_1 accounts for 54% of that of I .

The angle of the ascending node for the first case is $\Omega = 357^\circ.5 \pm 9^\circ.3$, and $\Omega = 220^\circ.3 \pm 9^\circ.3$ for the second. The semimajor axis obtained is $0''.1646 \pm 0''.0030$, and the sum of the masses is 1.62 ± 0.10 , being deduced from the expression (1). From this value and that of $\alpha = 1.57 \pm 0.27$, the individual masses: $M_1 = 0.99 \pm 0.09 M_\odot$ and $M_2 = 0.63 \pm 0.08 M_\odot$ are obtained for each component. Figure 2 represents the direct and retrograde motion orbits. In both cases, the dashes represent the now determined line of the nodes.

One can try different values of α and will observe that for values close to that selected, the individual masses yielded are compatible with the spectral types. However, the farther we move away from that value, the more we will obtain poorly adjusted masses. In Table 3 the solution for different values of the quotient of masses (α) can be seen.

In practice the algorithm can be designed to find the solution for a fixed step, which can be arbitrarily small. The flowchart of the algorithm can be seen in Fig. 3. As we can see in the diagram, we start with an initial value of the inclination I_0 , and we add the step ΔI until the difference between the calculated and the initial values of the inclination is lower than a given tolerance ϵ .

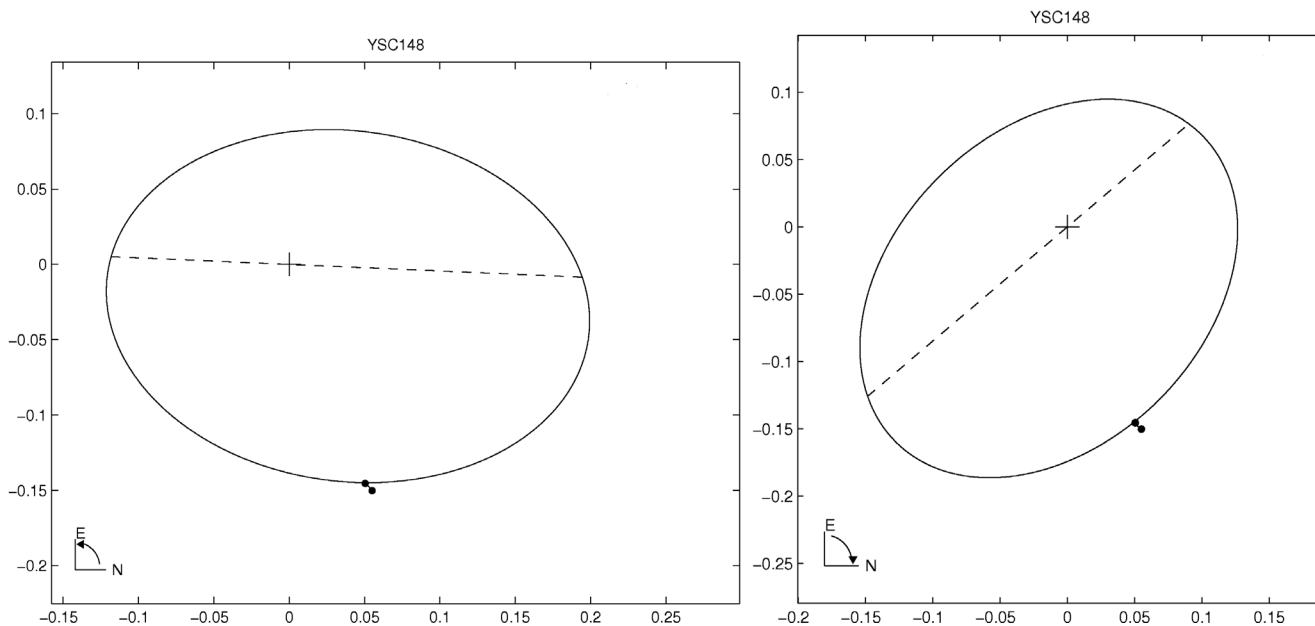


Fig. 2. Orbit of the system YSC 148, direct and retrograde motion.

3.2. System *CHR 225 = HD 34318 = HIP 24560 = WDS 05162-1121*

This SB1 has a spectroscopic orbit, calculated by [15], with the following elements:

$$\begin{aligned}
 P &= 3909.^{\text{d}}7 \pm 6.^{\text{d}}0 = 10.704 \pm 0.016 \text{ yr,} \\
 T &= 46423.9 \pm 5.9 \text{ RJD} = 2018.093 \pm 0.016, \\
 e &= 0.904 \pm 0.004, \\
 \bar{A}_1 &= 4.24305 \times 10^8 \pm 1.3 \times 10^7 \text{ km,} \\
 \omega_1 &= 32.^{\circ}0 \pm 1.^{\circ}4.
 \end{aligned}$$

Its combined spectrum is G0, and its Hipparcos parallax is $\pi = 4.38 \pm 0.45$. Nevertheless, in some catalogs, such as the All-Sky Compiled Catalogue of 2.5 million stars [16], it is listed as A2–3V/G8 III, while the authors of the orbit consider the spectra A3:/G8 III based on the work of [17]. Thus we consider two possible scenarios: one with a component pertaining to the main sequence and the other with both stars being of luminosity class III which corresponds to $\alpha = 0.77 (2.0/2.6) \pm 0.15$ in the first case and $\alpha = 0.88 (2.3/2.6) \pm 0.26$ in the second case.

Below, we show the two speckle measurements that exist for this binary, both obtained by [18]:

| t | θ , deg | ρ , arcsec | Δm |
|-----------|----------------|-------------------|------------|
| 1989.9387 | 51.6 ± 2.5 | 0.061 ± 0.003 | 0.6 |
| 1993.0923 | 55.7 ± 2.5 | 0.051 ± 0.003 | 0.6 |

The results obtained for each spectral type and each measurement are listed in Tables 4 and 5.

Taking into account the spectral types A3 V + G8 III, the residuals are:

| t | Direct motion | | Retrograde motion | |
|-----------|----------------------|-----------------------|----------------------|-----------------------|
| | $\Delta\theta$, deg | $\Delta\rho$, arcsec | $\Delta\theta$, deg | $\Delta\rho$, arcsec |
| 1989.9387 | -0.4 | 0.000 | -0.4 | 0.000 |
| 1993.0923 | -7.8 | -0.006 | 15.2 | -0.006 |

From Table 5 we can conclude that the first observation produces values of the masses that have a higher level of agreement with the spectra in both scenarios. This conclusion can explain the quite large residual for the second measurement.

On the other hand, the observational data would suggest as more probable the orbit with direct motion, which is represented in Fig. 4.

3.3. System *LSC 1 Aa1,2 = HD 200077 = HIP 103641 = WDS 20599+4016*

This system was recently resolved for the first time by [19] by means of speckle interferometry, with the following measurements:

| t | θ , deg | ρ , arcsec | Δm |
|-----------|-----------------|--------------------|------------|
| 2012.5738 | 257.8 ± 2.4 | 0.0218 ± 0.009 | 1.20 |
| 2012.5738 | 256.7 ± 2.4 | 0.0231 ± 0.009 | 1.21 |

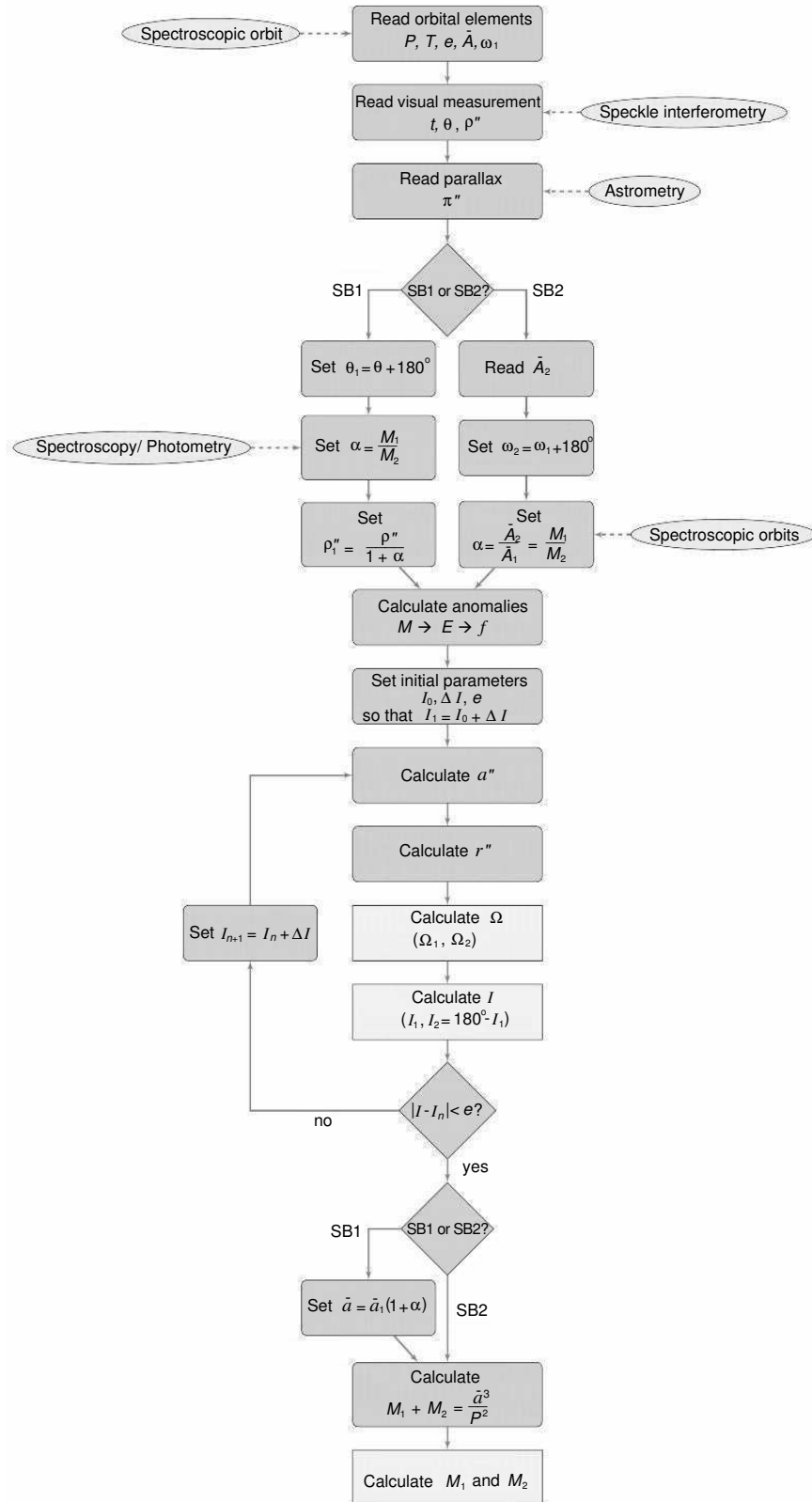


Fig. 3. Flowchart of the algorithm.

Table 4. Calculated orbital elements for the system CHR 225

| Spectral type | Observation | Final I , deg | Final $180^\circ - I$, deg | Ω for I , deg | Ω for $180^\circ - I$, deg | a , arcsec |
|---------------|-------------|-----------------|-----------------------------|------------------------|------------------------------------|---------------------|
| A3 V+ | 1989.9387 | 39 ± 10 | 141 ± 10 | 31 ± 20 | 73 ± 20 | 0.0349 ± 0.0022 |
| G8 III | 1993.0923 | 43.3 ± 6.8 | 136.7 ± 6.8 | 25 ± 13 | 87 ± 13 | 0.0320 ± 0.0020 |
| A3 III+ | 1989.9387 | 41.8 ± 9.5 | 138.2 ± 9.5 | 31 ± 22 | 72 ± 22 | 0.0351 ± 0.0021 |
| G8 III | 1993.0923 | 46.2 ± 6.2 | 133.8 ± 6.2 | 26 ± 15 | 85 ± 15 | 0.0324 ± 0.0019 |

Given that the observations are from the same epoch, we will use an average of both for the calculus.

A double lined spectroscopic orbit exists for this binary [20] that contains the following elements:

$$P = 112^{\text{d}}546 \pm 0^{\text{d}}036 = 0.30813 \pm 0.00010 \text{ yr},$$

$$T = 46517.6 \pm 0.089 \text{ RJD} \\ = 2013.04437 \pm 0.00024,$$

$$e = 0.6565 \pm 0.0038,$$

$$\bar{A}_1 = 3.38782 \times 10^8 \pm 410\,000 \text{ km},$$

$$\bar{A}_2 = 3.98203 \times 10^8 \pm 860\,000 \text{ km},$$

$$\omega_1 = 197^\circ 28 \pm 0^\circ 55.$$

In this case we have the quotient of the masses $\alpha = \bar{A}_2/\bar{A}_1 = M_1/M_2 = 1.18 \pm 0.07$ from the orbit

for which an *a priori* analysis of the spectral types and the differences of magnitude is not necessary. Applying the proposed methodology, the following results are obtained for this value of α using the Hipparcos parallax $\pi = 24.42 \pm 0.56 \text{ mas}$:

$$\begin{aligned} a'' &= 0''.01388 \pm 0''.00037, \\ I &= 60^\circ \pm 11^\circ, \text{ or } 120^\circ \pm 11^\circ, \\ \Omega &= 70^\circ \pm 21^\circ, \text{ or } 85^\circ \pm 21^\circ, \\ M_1 + M_2 &= 1.94 \pm 0.08 M_\odot, \\ M_1 &= 1.05 \pm 0.05 M_\odot, \\ M_2 &= 0.89 \pm 0.05 M_\odot. \end{aligned} \quad (3)$$

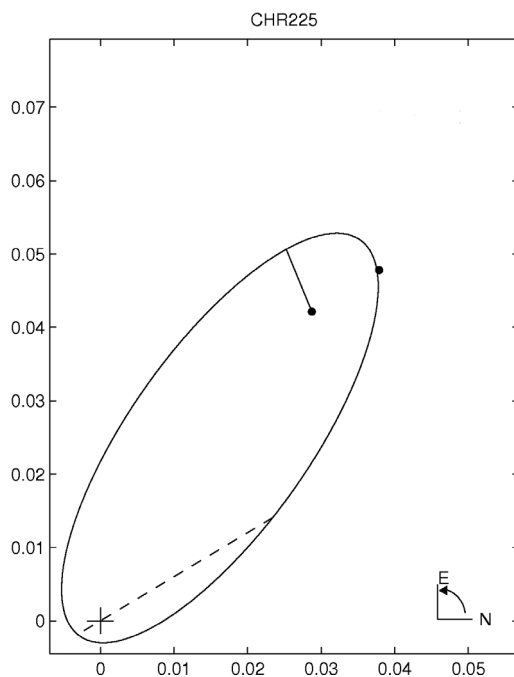
In addition, based on spectroscopic as well as astrometric measurements taken by the Palomar Testbed Interferometer, a tridimensional and precise orbit exists for this binary [21] that has the following elements:

$$\begin{aligned} P &= 112^{\text{d}}5132 \pm 0^{\text{d}}0013, \\ T &= 53830.169 \pm 0.014 \text{ MJD}, \\ e &= 0.66227 \pm 0.00051, \\ a &= 0''.014453 \pm 0''.000018, \\ I &= 118^\circ 682 \pm 0^\circ 080, \\ \Omega &= 89^\circ 403 \pm 0^\circ 028, \\ \omega &= 197^\circ 072 \pm 0^\circ 025. \end{aligned}$$

This orbit is very similar to one of those obtained (retrograde motion) in the present article which demonstrates the efficiency of the proposed algorithm. In this concrete case, given that the direction of motion is known, the correct values in (3) will be $I = 120^\circ \pm 11^\circ$ and $\Omega = 85^\circ \pm 21^\circ$.

3.4. System Mkt 11 Aa, Ab = HD 358 = HIP 677 = WDS 00084+2905

With the objective of testing the proposed algorithm again, we have selected an SB2 with an orbit

**Fig. 4.** Orbit of the system CHR 225.

that, moreover, has a retrograde spectro-interferometric orbit [22] based on an ample set of speckle observations [23]. The complete set of elements follows.

Spectroscopic orbit:

$$\begin{aligned}
 P &= 96^{\text{d}}7005 \pm 0^{\text{d}}00438291 \\
 &= 0.26476 \pm 0.00001 \text{ yr}, \\
 T &= 47374.6 \pm 0.0921029 \text{ RJD} \\
 &= 1988.5831 \pm 0.00025, \\
 e &= 0.534812 \pm 0.0046, \\
 \bar{A}_1 &= 3.11731 \times 10^7 \pm 630000 \text{ km}, \\
 \bar{A}_2 &= 7.35554 \times 10^7 \pm 1.1 \times 10^6 \text{ km}, \\
 \omega_1 &= 77^{\circ}4527 \pm 0^{\circ}31.
 \end{aligned}$$

Spectro-interferometric orbit:

$$\begin{aligned}
 P &= 96^{\text{d}}7015 \pm 0^{\text{d}}0044 \\
 &= 0.26476 \pm 0.00012 \text{ yr}, \\
 T &= 47374.563 \pm 0.095 \text{ RJD} \\
 &= 1988.5830 \pm 0.0003, \\
 e &= 0.535 \pm 0.0046, \\
 a'' &= 0''.024 \pm 0''.00013, \\
 I &= 105^{\circ}6 \pm 0^{\circ}23, \\
 \Omega &= 284^{\circ}4 \pm 0^{\circ}21, \\
 \omega &= 257^{\circ}4 \pm 0^{\circ}31.
 \end{aligned}$$

The parallax of this system, measured by Hipparcos, is $\pi = 33.62 \pm 0.35$ mas.

Given that the first two on the available list of speckle observations correspond to the same epoch, we will take the average of them in order to apply our methodology:

| t | θ , deg | ρ , arcsec | Δm |
|-----------|----------------|-----------------|----------------|
| 1988.6880 | 256.78 | 0.01828 | 1.90 ± 0.4 |
| | ± 0.72 | ± 0.00032 | |

With that data and with $\alpha = \bar{A}_2/\bar{A}_1 = 2.36 \pm 0.52$,

Table 5. Calculated masses for the system CHR 225

| Spectral type | Observation | M_1, M_{\odot} | M_2, M_{\odot} |
|---------------|-------------|------------------|------------------|
| A3 V+ | 1989.9387 | 1.92 ± 0.26 | 2.50 ± 0.29 |
| G8 III | 1993.0923 | 1.48 ± 0.20 | 1.93 ± 0.22 |
| A3 III+ | 1989.9387 | 2.11 ± 0.36 | 2.38 ± 0.37 |
| G8 III | 1993.0923 | 1.66 ± 0.28 | 1.88 ± 0.29 |

the following results are obtained:

$$\begin{aligned}
 a'' &= 0''.02443 \pm 0''.00039, \\
 I &= 74^{\circ}50 \pm 0^{\circ}37 \text{ or } 105^{\circ}5 \pm 0^{\circ}37, \\
 \Omega &= 228^{\circ}3 \pm 2^{\circ}5 \text{ or } 285^{\circ}2 \pm 2^{\circ}5, \\
 M_1 + M_2 &= 5.47 \pm 0.20, \\
 M_1 &= 3.84 \pm 0.29 M_{\odot}, \\
 M_2 &= 1.63 \pm 0.26 M_{\odot}.
 \end{aligned}$$

With the objective of comparing the values of I , Ω , and a as well as the masses obtained from each available observation, it is interesting to give the corresponding results presented in Table 6.

The results are very similar among themselves; although, in some cases, the uncertainties in I and Ω are high. This is due to the proximity of the measurement to the nodes, as previously commented. Such is the case of that which corresponds to $t = 1989.6708$, with a position angle of $\theta = 284^{\circ}9$, for which the result of the ascending node is $\Omega = 284^{\circ}5$. In the same case, it would be that of $t = 1989.6735$, with $\theta = 283^{\circ}59$ and $\Omega = 284^{\circ}2$. Close to the descending node, we have $t = 1989.6243$, with $\theta = 102^{\circ}98$ and $\Omega = 283^{\circ}4$. A spectrum of B8 IVp is assigned in the Washington Catalog [24] which would be in agreement with our calculation of masses, although Abt considers B9 II [25]. Nevertheless, if we calculate its absolute magnitude by means of the Hipparcos parallax [26] and the observed visual magnitude, that would give us a value of -0.3 , which does not correspond to a giant of luminosity class II and, instead, it could correspond to a luminosity class IV.

4. CONCLUSIONS

In this article we present proof that it is possible to obtain the inclination, the ascending node, and the semimajor axis of spectroscopic binary orbits by additionally using a single quality observation that yields the relative position of the pair (θ, ρ) as well as the parallax (π) , that is to say, the three-dimensional orbit

Table 6. Results with different measurements for the system Mkt 11 Aa, Ab

| t | I , deg | Ω , deg | a , arcsec | M_1, M_\odot | M_2, M_\odot |
|-----------|--------------------|-------------------|-----------------------|-----------------|-----------------|
| 1988.6880 | 105.5 \pm 0.37 | 285.2 \pm 2.5 | 0.02443 \pm 0.00039 | 3.84 \pm 0.29 | 1.63 \pm 0.26 |
| 1988.6906 | 105.75 \pm 0.43 | 285.1 \pm 3.1 | 0.02445 \pm 0.00039 | 3.86 \pm 0.29 | 1.63 \pm 0.26 |
| 1988.7533 | 106.28 \pm 3.25 | 279.6 \pm 4.1 | 0.02452 \pm 0.00039 | 3.89 \pm 0.29 | 1.65 \pm 0.26 |
| 1988.7562 | 105.50 \pm 1.18 | 284.4 \pm 2.1 | 0.02442 \pm 0.00039 | 3.84 \pm 0.29 | 1.63 \pm 0.26 |
| 1988.7588 | 106.10 \pm 0.82 | 283.7 \pm 1.7 | 0.02450 \pm 0.00039 | 3.88 \pm 0.29 | 1.64 \pm 0.26 |
| 1988.8108 | 100.67 \pm 0.48 | 288.6 \pm 8.7 | 0.02395 \pm 0.00038 | 3.62 \pm 0.27 | 1.54 \pm 0.25 |
| 1988.8136 | 104.10 \pm 0.45 | 285.1 \pm 7.1 | 0.02427 \pm 0.00039 | 3.77 \pm 0.28 | 1.60 \pm 0.26 |
| 1988.8164 | 102.22 \pm 1.03 | 286.3 \pm 12.2 | 0.02408 \pm 0.00038 | 3.68 \pm 0.28 | 1.56 \pm 0.25 |
| 1988.8192 | 103.96 \pm 0.64 | 284.9 \pm 10.4 | 0.02425 \pm 0.00039 | 3.76 \pm 0.28 | 1.59 \pm 0.26 |
| 1989.6161 | 101.42 \pm 2.00 | 285.7 \pm 27.0 | 0.02401 \pm 0.00038 | 3.65 \pm 0.28 | 1.55 \pm 0.25 |
| 1989.6243 | 103.64 \pm 25.03 | 283.4 \pm 309.5 | 0.02422 \pm 0.00039 | 3.75 \pm 0.28 | 1.59 \pm 0.25 |
| 1989.6544 | 104.49 \pm 0.72 | 285.3 \pm 6.7 | 0.02431 \pm 0.00039 | 3.79 \pm 0.29 | 1.61 \pm 0.26 |
| 1989.6654 | 102.4 \pm 0.95 | 285.3 \pm 22.2 | 0.02406 \pm 0.00038 | 3.67 \pm 0.29 | 1.56 \pm 0.26 |
| 1989.6735 | 101.6 \pm 4.79 | 284.2 \pm 107.0 | 0.02403 \pm 0.00038 | 3.66 \pm 0.28 | 1.55 \pm 0.25 |
| 1989.6791 | 102.98 \pm 1.01 | 284.0 \pm 22.9 | 0.02415 \pm 0.00039 | 3.72 \pm 0.28 | 1.57 \pm 0.25 |
| 1989.6818 | 103.33 \pm 0.94 | 283.9 \pm 17.8 | 0.02419 \pm 0.00039 | 3.73 \pm 0.28 | 1.58 \pm 0.25 |
| 1989.6874 | 102.56 \pm 0.86 | 283.1 \pm 15.5 | 0.02411 \pm 0.00038 | 3.70 \pm 0.28 | 1.57 \pm 0.25 |
| 1989.6901 | 103.39 \pm 0.47 | 283.5 \pm 9.9 | 0.02419 \pm 0.00039 | 3.73 \pm 0.28 | 1.58 \pm 0.25 |
| 1989.7637 | 105.51 \pm 0.50 | 284.7 \pm 2.4 | 0.02443 \pm 0.00039 | 3.84 \pm 0.29 | 1.63 \pm 0.26 |
| 1989.7664 | 104.22 \pm 0.70 | 280.4 \pm 3.3 | 0.02428 \pm 0.00039 | 3.77 \pm 0.28 | 1.60 \pm 0.26 |

Table 7. Inclinations, nodes, semimajor axes, and masses obtained for the four examples studied

| System | I , deg | Ω , deg | a , arcsec | M_1, M_\odot | M_2, M_\odot |
|-------------------------|------------------|-----------------|-----------------------|-----------------|-----------------|
| YSC 148 (Direct) | 43 \pm 28 | 357.5 \pm 9.3 | 0.1646 \pm 0.0030 | 0.99 \pm 0.09 | 0.63 \pm 0.08 |
| YSC 148 (Retrograde) | 137 \pm 28 | 220.3 \pm 9.3 | 0.1646 \pm 0.0030 | 0.99 \pm 0.09 | 0.63 \pm 0.08 |
| CHR 225 | 39 \pm 10 | 31 \pm 20 | 0.0349 \pm 0.0022 | 1.92 \pm 0.26 | 2.50 \pm 0.29 |
| LSC 1 Aa1,2 | 120 \pm 11 | 85 \pm 21 | 0.01388 \pm 0.00037 | 1.05 \pm 0.05 | 0.89 \pm 0.05 |
| Mkt 11 Aa, Ab | 105.5 \pm 0.37 | 285.2 \pm 2.5 | 0.02443 \pm 0.00039 | 3.84 \pm 0.29 | 1.63 \pm 0.26 |

of the binary is obtained. Moreover, an estimation of the individual masses is also possible.

This is feasible due to the establishment of an original analytic algorithm in which, beginning with the orbital inclination, one arrives again at the same orbital element at the end of the calculation process.

In this way, we obtain the maximum amount of information regarding these binary systems even before having calculated the visual orbit.

The practical utility of the procedure is shown in the examples used in the cases of the SB1s: YSC 148 = HD 37393 and CHR 225 = HD 34318, as well as of the SB2s: LSC 1 Aa1,2 = HD 200077 and Mkt 11 Aa, Ab = HD 358. For the first two binaries, new information was obtained. The last two were selected because they both have a spectroscopic as well as an astrometric orbit. In this manner, we have established that the deduced results are in agreement with those obtained by following our methodology.

For all of the examples presented here (summarized in Table 7), we kept in mind the propagation of uncertainties with the objective of presenting our results along with the corresponding uncertainties.

The generally useful methodology is especially interesting to apply to those systems for which the telescope was able to resolve the binary only at the maximum angular separation. It may also provide a way to evaluate the accuracy of the astrometric measurements, comparing the results obtained using them with those provided by other measurements, as seen in Table 6.

ACKNOWLEDGMENTS

This research was financed by the AYA 2011-26429 project of the Spanish Ministerio de Ciencia e Innovación and by a grant from IeMath-Galicia (FEDER-Xunta de Galicia, Spain). We made use of the following catalogs: the Washington Double Star Catalog and the Fourth Catalog of Interferometric Measurements of Binary Stars (WDS and INT4, the US Naval Observatory); the R. M. Aller Astronomical Observatory Catalog of Orbits and Ephemerids of Visual Double Stars (OARMAC, J. A. Docobo, J. F. Ling and P. P. Campo); The Ninth Catalogue of Spectroscopic Binary Orbits (SB9, D. Pourbaix et al.); the Hipparcos Catalog, New Reduction (F. van Leeuwen); the All-Sky Compiled Catalogue of 2.5 million stars (ASCC-2.5, 3rd version, N. V. Kharchenko and S. Roeser).

REFERENCES

1. V. Straizys and G. Kuriliene, *Astrophys. and Space Sci.* **80**, 353 (1981).
2. D. F. Gray, *The Observation and Analysis of Stellar Photospheres* (Cambridge Univ. Press, 2005).
3. J. A. Docobo and M. Andrade, *Astrophys. J.* **652**, 681 (2006).
4. J. W. Davidson, Jr., B. J. Baptista, E. P. Horch, et al., *Astron. J.* **138**, 1354 (2009).
5. A. Labeyrie, *Astron. and Astrophys.* **6**, 85 (1970).
6. A. Labeyrie, D. Bonneau, R. V. Stachnik, and D. Y. Gezari, *Astrophys. J. Lett.* **194**, L147 (1974).
7. K. T. Knox and B. J. Thompson, *Astrophys. J. Lett.* **182**, L133 (1973).
8. H. A. McAlister, *Publ. Astron. Soc. Pacific* **88**, 317 (1976).
9. H. A. McAlister, *Publ. Astron. Soc. Pacific* **88**, 957 (1976).
10. Y. Y. Balega and N. A. Tikhonov, *Sov. Astron. Lett.* **3**, 272 (1977).
11. Y. Y. Balega and V. P. Ryadchenko, *Sov. Astron. Lett.* **10**, 95 (1984).
12. J. B. Breckinridge, H. A. McAlister, and W. G. Robinson, *Appl. Opt.* **18**, 1034 (1979).
13. D. W. Latham, R. P. Stefaniz, G. Torres, et al., *Astron. J.* **124**, 1144 (2002).
14. E. P. Horch, L. A. P. Bahi, J. R. Gaulin, et al., *Astron. J.* **143**, 10 (2012).
15. J. M. Carquillat and J. L. Prieur, *Astronomische Nachrichten* **328**, 527 (2007).
16. N. V. Kharchenko, *Kinematika i Fizika Nebesnykh Tel* **17**, 409 (2001).
17. N. Ginestet and J. M. Carquillat, *Astrophys. J. Suppl.* **143**, 513 (2002).
18. W. I. Hartkopf, B. D. Mason, H. A. McAlister, et al., *Astron. J.* **111**, 936 (1996).
19. E. P. Horch, S. B. Howell, M. E. Everett, and D. R. Ciardi, *Astron. J.* **144**, 165 (2012).
20. D. Goldberg, T. Mazeh, D. W. Latham, et al., *Astron. J.* **124**, 1132 (2002).
21. M. Konacki, M. W. Muterspaugh, S. R. Kulkarni, and K. G. Helminiak, *Astrophys. J.* **719**, 1293 (2010).
22. D. Pourbaix, *Astron. and Astrophys. Suppl.* **145**, 215 (2000).
23. X. Pan, M. Shao, M. M. Colavita, et al., *Astrophys. J.* **384**, 624 (1992).
24. B. D. Mason, G. L. Wycoff, W. I. Hartkopf, et al., *Astron. J.* **122**, 3466 (2001).
25. H. A. Abt, *Astrophys. J. Suppl.* **180**, 117 (2009).
26. F. van Leeuwen, *Astron. and Astrophys.* **474**, 653 (2007).